Original Research

Prenatal indole-3-carbinol administration activates aryl hydrocarbon receptor-responsive genes and attenuates lung injury in a bronchopulmonary dysplasia model

Gabriela Guzmán-Navarro[1],*, Mario Bermúdez de León[2], Irene Martín-Estal[1],
Raquel Cuevas-Díaz Durán[1], Laura Villarreal-Alvarado[1], Anakaren Vaquera-Vázquez[1],
Tania Cuevas-Cerda[1], Karina Garza-García[1], Luis Eduardo Cuervo-Pérez[3],
Álvaro Barbosa-Quintana[3], José Eduardo Pérez-Saucedo[1], Víctor J Lara-Díaz[1] (iD) and
Fabiola Castorena-Torres[1],* (iD)

[1]Tecnológico de Monterrey, Escuela de Medicina y Ciencias de la Salud, Monterrey 64710, Mexico; [2]Departamento de Biología Molecular, Centro de Investigación Biomédica del Noreste, Instituto Mexicano del Seguro Social, Monterrey 64720, Mexico; [3]Hospital San José, Sistema de Salud del Tecnológico de Monterrey, Monterrey 64710, Mexico
Corresponding author: Fabiola Castorena-Torres. Email: fcastorena@tec.mx
*These authors contributed equally to this work

Impact statement

Broncopulmonary dysplasia (BPD) is developed by preterm infants when they are exposed to hyperoxia–hypoxia cycles. To search new effective and innocuous therapeutic options to decrease the damage caused by supplemental oxygen is one of goals in BPD treatment. In our study, using an animal model, we have shown a beneficial effect of indole-3-carbinol (I3C), a cruciferous vegetable derivative, to treat BPD. I3C can diffuse through the placental membrane and activates the antioxidant system in fetuses. I3C reduces the destruction of alveolar septa and reduces fibrosis in pup lungs. This information provides the basis for the use of innocuous molecules contained in plants to prevent BPD in those babies from women with high risk to get preterm delivery.

Abstract

Hyperoxia−hypoxia exposure is a proposed cause of alveolar developmental arrest in bronchopulmonary dysplasia in preterm infants, where mitochondrial reactive oxygen species and oxidative stress vulnerability are increased. The aryl hydrocarbon receptor (AhR) is one of the main activators of the antioxidant enzyme system that protects tissues and systems from damage. The present study aimed to determine if the activation of the AhR signaling pathway by prenatal administration of indole-3-carbinol (I3C) protects rat pups from hyperoxia–hypoxia-induced lung injury. To assess the activation of protein-encoding genes related to the AhR signaling pathway (*Cyp1a1*, *Cyp1b1*, *Ugt1a6*, *Nqo1*, and *Gsta1*), pup lungs were excised at 0, 24, and 72 h after birth, and mRNA expression levels were quantified by reverse transcription-quantitative polymerase chain reaction assays (RT-qPCR). An adapted Ratner's method was used in rats to evaluate radial alveolar counts (RACs) and the degree of fibrosis. The results reveal that the relative expression of AhR-related genes in rat pups of prenatally I3C-treated dams was significantly different from that of untreated dams. The RAC was significantly lower in the hyperoxia–hypoxia group (4.0 ± 1.0) than that in the unexposed control group (8.0 ± 2.0; $P < 0.01$). When rat pups of prenatally I3C-treated dams were exposed to hyperoxia–hypoxia, an RAC recovery was observed, and the fibrosis index was similar to that of the unexposed control group. A cytokine antibody array revealed an increase in the NF-κB signaling cascade in I3C-treated pups, suggesting that the pathway could regulate the inflammatory process under the stimulus of this compound. In conclusion, the present study demonstrates that I3C prenatal treatment activates AhR-responsive genes in pup's lungs and hence attenuates lung damage caused by hyperoxia–hypoxia exposure in newborns.

Keywords: Bronchopulmonary dysplasia, hyperoxia–hypoxia, aryl hydrocarbon receptor, indole-3-carbinol, murine model, newborns

Introduction

Bronchopulmonary dysplasia (BPD) is the most common chronic respiratory disease in preterm infants and is a major form of neonatal chronic lung disease.[1] Exposure to supraphysiological oxygen levels is a proposed cause of alveolar developmental arrest in BPD. Intermittent periods of hypoxia increase mitochondrial reactive oxygen species (ROS) production and tissue vulnerability to oxidative stress, leading to alveolar cell injury in developing lungs. Additionally, antioxidant deficiencies and immature defenses increase the risk of irreversible lung damage.[2–4] In a neonatal murine model that mimics human infant development, brief episodes of oxygen desaturation exacerbated oxidative stress during the initial stages of BPD.[5] Pulmonary morphological changes, including larger alveoli, a decreased alveolar number, and increased interstitial thickness, accompany the aforementioned oxidative stress events. All these alterations are consistent with those found in BPD in human neonates.[6]

One protein responsible for a cell's antioxidant system is the aryl hydrocarbon receptor (AhR). This molecule has several endogenous and exogenous ligands and is located in the cytoplasm, where it interacts with chaperones: two 90 kDa heat shock transcriptional regulators,[6–9] a co-chaperone (p23), and a single molecule of the hepatitis X-associated protein-2.[10,11] After being stimulated, the AhR exposes a nuclear localization sequence that translocates the AhR complex (formed by AhR/aryl hydrocarbon receptor nuclear translocator) into the nucleus.[12,13] Here, the AhR dissociates and dimerizes with the AhR nuclear translocator, activating all genes with xenobiotic response elements.[14] Most of these genes encode phase I and phase II antioxidant enzymes, such as cytochrome P450 (CYP450) members, glutathione S-transferase α, and NAD(P)H quinone reductase-1 (NQO1).[15–19] Some of these genes are also regulated by the nuclear factor erythroid-derived 2 (Nrf2) via antioxidant response elements as a reply to oxidative stress.[20] It has been demonstrated that both adult and newborn mice deficient in the AhR have a greater susceptibility to lung lesions because of hyperoxia due to the low or null expression of phase I and phase II antioxidant enzymes.[19,21,22] These results suggest that the AhR is important in the protection of the lungs from oxygen-induced injury.

Recently, several studies have proposed different phytochemicals derived from fruits or vegetables as an adjuvant treatment for BPD. Vitamin A is involved in the proliferation and maintenance of epithelial cells, and it is necessary for both cellular differentiation and surfactant production within the lung but only had a modest benefit in reducing BPD risk among preterm infants.[23] Regarding the use of different sources of intravenous fat, a study comparing soy oil emulsion-based with mixed oil sources failed to reach a significant difference in the incidence of BPD; moreover, in the study conducted by Guthrie *et al.* in 2017, the soy oil emulsion-based group showed a 46% BPD incidence, whereas the mixed oil-based group had a 24% BPD incidence.[24] Additionally, indole-3-carbinol (I3C) is a cruciferous vegetable derivative that can induce phase I

and phase II drug-metabolizing enzymes, anti-oxidative stress responses, the anti-inflammatory NF-κB signaling pathway, and cell cycle arrest and apoptosis.[25] It has been recently reported that I3C suppresses inflammation-driven lung cancer in mice and acts as a potent inhibitor of ischemia–reperfusion-induced inflammation, but this effect has never been evaluated in the context of BPD.[26] For this reason, I3C could help to reduce the deleterious effects observed in neonates exposed to hyperoxia–hypoxia cycles, in which several inflammatory and anti-inflammatory cytokines have demonstrated an important role in the immunomodulation of lung damage.[27,28]

In the present study, we used a BPD rat model to determine if I3C prenatal administration would activate the AhR signaling pathway in neonatal pups, thus protecting them from hyperoxia–hypoxia-induced lung injury.

Materials and methods

Chemicals

I3C (I7256) was purchased from Sigma-Aldrich (St. Louis, MO, USA).

Animals

Sprague Dawley pregnant rats (Harlan Laboratories, Bar Harbor, ME, USA) were housed in normal conditions with 12:12 h light–dark cycles. All animals had *ad libitum* access to food and water, and body weight and food intake were recorded daily. The animals were handled according to the protocol approved by the Institutional Animal Care and Use Committee at the Tecnologico de Monterrey (ID: 2015-Re-015), in full compliance with the Official Mexican Standard (NOM-062-ZOO-1999) for the production, care, and use of laboratory animals for scientific purposes.

Animal treatment

Pregnant rats were treated daily with I3C by oral gavage (100 mg/kg body weight) suspended in 0.5 mL of corn oil (as a vehicle) daily, starting on day 17 of gestation until birth (day 21). Control rats from all groups received corn oil as a vehicle. Two pregnant rats were handled simultaneously at the same time, starting with the control group, then the exposed group and finally with the exposed group treated with I3C. Pups from multiple litters were pooled before being randomly assigned and redistributed to dams. A total of 79 pups were divided as follows: to validate the AhR activation in pup's lungs, into a control group ($n = 15$) and an I3C-treated group ($n = 15$); to measure an array of cytokines in plasma, into a control group ($n = 9$, spots by duplicates), a hyperoxia–hypoxia group ($n = 6$, spots by duplicates), and an I3C-treated exposed group ($n = 6$, spots by duplicates); and to test the BDP model through histopathology, either for radial alveolar count (RAC) or fibrosis index or both, into a control group ($n = 10$), a hyperoxia–hypoxia group ($n = 11$), and an I3C-treated exposed group ($n = 7$). Nurse rats were euthanized with intraperitoneal sodium pentobarbital (150 mg/kg), according the AVMA Guidelines for the Euthanasia of

Animals: 2013 Edition. Absence of corneal reflex and absence of rhythmic breathing were used as a confirmatory method of euthanasia.[29] All pups were deeply anesthetized according to guidelines published by Institutional Animal Care and Use Committee of the University of Iowa[30] at 0, 24 and 72 h after birth, and blood was extracted by intracardiac puncture and lungs were dissected. These tissues were preserved either in RNA later for RT-qPCR analyses or PBS-formalin for histological analyses.

BPD model

BDP in neonatal rats was developed based on Ratner's method.[5,31] From the second postnatal day, pups were exposed to 80% oxygen in a chamber designed at the Laboratory Center for Research and Innovation in Health (Escuela de Medicina y Ciencias de la Salud, Tecnologico de Monterrey). A Respironics EverFlo-OPI oxygen concentrator (120v-Millennium Technology 60 GHz, 3.4A) generated the oxygen flow. An oxygen sensor (Lutron model DO-5510HA COD meter) was installed to constantly monitor the oxygen concentration inside the chamber. The experimental model is illustrated in Figure 1. Hyperoxia exposure was interrupted with intermittent exposure to hypoxic stress at 10% oxygen for 10 min (N_2 balanced) and air at 21% oxygen for 50 min to clean the cages once a day, in continuous and intermittent episodes until the 13th day. To reduce the use of mothers exposed to supplemental oxygen, a nurse attended the experimental litter in alternate 24 h shifts.

RNA isolation, cDNA synthesis, and real-time RT-qPCR assays

The lungs stored in RNAlater were subject to total RNA extraction using the TRIzol reagent (Invitrogen, Carlsbad, CA, USA) according to the manufacturer's instructions. RNA concentration and purity were estimated by UV spectrophotometry using a Nanodrop 2000 (Thermo Scientific, Wilmington, DE, USA), and RNA integrity was assessed by electrophoresis on 1% agarose gels stained with GelRed (Biotium, Landing Parkway Fremont, CA, USA). Isolated RNA was stored at $-80°C$ until analysis.

Then, cDNA was prepared from 500 ng of the total RNA using the SuperScript III First-Strand Synthesis System (Invitrogen) according to the manufacturer's instructions.

TaqMan Universal PCR Master Mix (Perkin Elmer, Foster City, CA, USA) was used for the PCR analyses, in a total volume of 20 μL containing 400 pmol/L of each oligonucleotide and 200 pmol/L of TaqMan probes. The assays were performed in a 96-well reaction plate on a Quant Studio 5.0 thermocycler (Applied Biosystems, Foster City, CA, USA). Ribosomal 18S RNA was used as an endogenous control (Applied Biosystems). The specific primers and probes related to the AhR signaling pathway were selected from the Thermo Scientific webpage
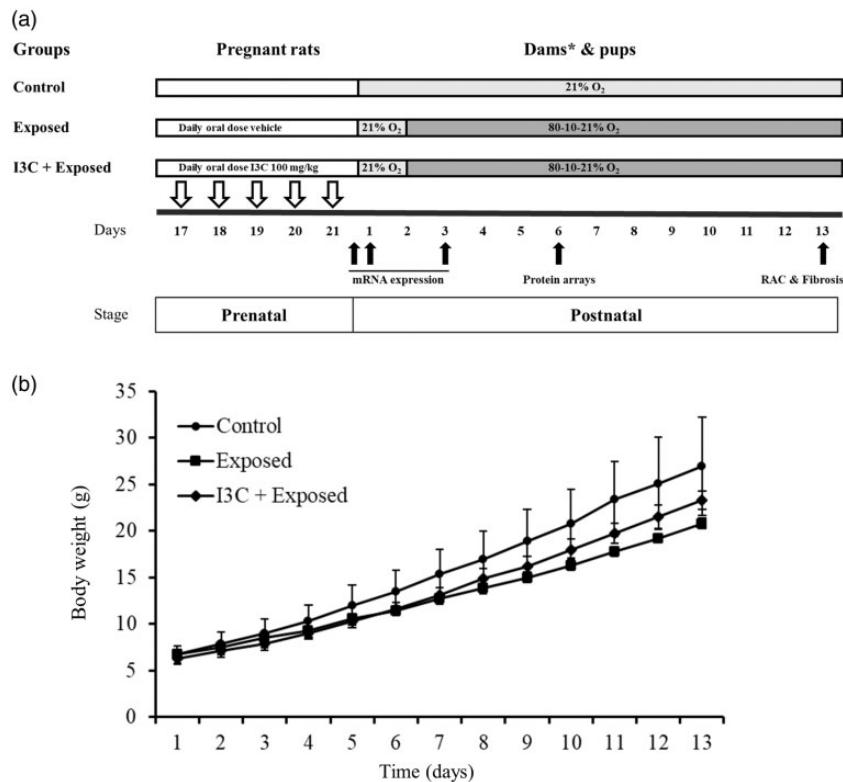
Figure 1. Effect of indole-3-carbinol (I3C) on newborn rat body weights. (a) Study design of the experimental model: control group (air environment: 21% O_2; $n = 10$), untreated exposed group (80%–10%–21% O_2; $n = 11$), and exposed group treated with I3C (100 mg/kg; 80%–10%––1% O_2; $n = 7$). For more details, see the Material and methods section. *Dams were changed on alternate days and all control groups received daily corn oil as a vehicle. (b) Body weight gain of newborn rats was evaluated daily for 13 days after birth. $P < 0.05$ control group vs. exposed group; $P > 0.05$ exposed group vs. I3C + exposed group.

(https://www.thermofisher.com/mx/es/home/life-science /pcr/real-time-pcr/real-time-pcr-assays/taqman-gene-expr ession.html; Table 1). Thermal cycling was performed with an initial incubation at 50°C for 2 min and then denatured at 95°C for 10 min, followed by 35 cycles. Each cycle consisted of heating at 95°C for 15 s for denaturalization and then 1 min at 60°C for annealing and extension. Each sample was run in triplicate, and negative controls were included in the same plate. Results were analyzed using the comparative threshold cycle method for relative gene expression.[32]

Cytokine protein array

A rat cytokine antibody array membrane (ab133992, Abcam, Cambridge, UK) was used to detect cytokines in plasma samples (from a pool of two or three pups) at day 6. Arrays contain spots by duplicate for each cytokine. The membrane was incubated for 30 min at 4°C in a blocking buffer. Then, samples were incubated on the membrane overnight at 4°C and were washed in buffer I for 5 min, followed by two washes in buffer II (5 min each). A biotinylated anti-cytokine mix of antibodies (1:2 000) was added to the membrane and incubated for 2 h. The membrane was washed and incubated with horseradish peroxidase-conjugated streptavidin (1:1 000) for 2 h before being incubated in 500 μL of detection buffer for 2 min and was then finally exposed to Kodak BioMax Light film (Sigma) at room temperature for 1 min. The chemiluminescent signal from bound cytokines was captured by the ChemiDoc MP Imaging System (Bio-Rad, CA, USA) and stored as a high-resolution TIFF image. ImageJ software was used to obtain cytokine signal intensities.

ImageJ scripts were developed for automated spot location and image processing. For each spot, raw intensity values were determined as the summed signal intensity of pixel values above a background correction threshold. Background correction thresholds were determined for each spot as the mean intensity values of the pixels in the corners of the square in which each spot was inscribed. Spot intensity values were further processed by subtracting the mean intensity values of the blank spots corresponding to each row. Background-corrected spot values were normalized using the positive control spots' mean intensities found in the control membrane, which was selected as the reference array.

Gene set enrichment analysis

A compendium of gene sets, including canonical pathways and gene ontologies, were downloaded from MsigDB 3 (http://software.broadinstitute.org/gsea/msigdb). Gene symbols corresponding to differentially expressed cytokines were used to find enriched gene sets through a hypergeometric test (R's phyper function). Gene sets were considered enriched if they had a P value of <0.05 and at least four genes.

Pulmonary histopathology

All the pups were deeply anesthetized and then perfused with a formalin solution (Sigma, St. Louis, MO, USA) by intracardiac puncture at 13th day, because is the common timeframe of saccular to alveolar development in rats, similar to preterm human infants.[6] Next, the trachea was cannulated with an 18 G catheter (Introcan Safety, Braun, Germany) connected to a three-way stopcock and a central venous pressure measuring tube (Manometer Set, Smiths Medical, USA), which had been filled with PBS-formalin. The lungs were gently expanded with the formalin solution until reaching a stable pressure of 20 cmH$_2$O. The tracheas were ligated, and each cardiopulmonary block was carefully dissected, excised, and immersed in a vial of PBS-formalin and then processed for routine paraffin embedding. Five-micrometer thick sections were obtained from the frontal plane of both lungs. Histological findings consistent with the microscopic description of bronchopulmonary dysplasia were intentionally sought; i.e., alveolar spaces enlarged by the destruction of alveolar septa,[33] interstitial and alveolar infiltrate of inflammatory cells such as lymphocytes, macrophages, and neutrophils, bronchiolar hyperplasia determined by an increase in squamous cells that limit the internal surface of the bronchioles,[34] and defined peribronchial edema with an excessive amount of fluid in the peribronchial interstitial tissue.[35]

Radial alveolar count

Digital images were obtained from sections stained with hematoxylin and eosin using an Infinity1 camera (Lumenera Corporation, Ottawa, ON, USA) connected to an Axio ImagerZ1 light microscope (Zeiss Microscopy, Oberkochen, Germany) at a magnification of 10×. In total, 560 areas were examined, 20 from each pup. The degree of alveolarization was measured by calculating the RAC according to the method established by Emery and

Table 1. Genes of cognate mRNAs quantified by RT-qPCR in this study.

Gene symbol	Gene name	Reference[a]
AhR	Aryl hydrocarbon receptor	Rn00565750_m1
Cyp1a1	Cytochrome P450, family 1, subfamily a, polypeptide 1	Rn00487218_m1
Cyp1b1	Cytochrome P450, family 1, subfamily b, polypeptide 1	Rn00564055_m1
Nqo1	NAD(P)H dehydrogenase 1, quinone 1	Rn00566528_m1
Ugt1a6	UDP glucuronosyltransferase 1 family, polypeptide A6	Rn00756113_m1
Aldh1a1	Aldehyde dehydrogenase 1 family, member A1	Rn00755484_m1
Aldh3a1	Aldehyde dehydrogenase 3 family, member A1	Rn00694669_m1
Gsta1	Glutathione S-transferase A1 (alpha-class GST)	Rn01757146_m1

[a]https://www.thermofisher.com/mx/es/home/life-science/pcr/real-time-pcr/real-time-pcr-assays/taqman-gene-expression.html

Mithal.[36] An investigator blind to the study group examined the digital images twice to determine the RAC. Any RAC values that did not match both examinations were reviewed a third time. The RAC was evaluated as the number of closed alveoli transected by a line drawn perpendicular to the terminal bronchiole toward the nearest pleura. Histological evidence of tissue injury was positive if one of the following was observed: (1) accumulation of neutrophils in the alveolar or interstitial space, (2) thickening of the alveolar wall, or (3) evidence of hemorrhaging or atelectasis.[37]

Mean linear intercept

Digital images of the hematoxylin and eosin stained lung sections were obtained using an AxioCam HRm camera (Zeiss Miccroscopy) connected to an Axio ImageZ1 light microscope at $10\times$ magnification. We use the semi-automated method proposed by Crowley *et al.*[38] to assess the mean free distance between gas exchange surfaces in the acinar airway complex. A set of images of 800×600 pixels were generated; fields with not entirely tissue were excluded. Five images per individual and three individuals per group were included in the analysis. On average 1093 chords per image and 5469 per lung were assessed using the protocol for semi-automated quantification using ImageJ program with an overlaid of 20 semi-transparent horizontal and 20 semi-transparent vertical lines. Based on the described method, the number and size of the alveolar were determined.

Analysis of fibrosis

The degree of fibrosis in the lungs was evaluated using paraffin sections stained with Masson's trichrome. Samples were systematically scanned in a microscope using a $20\times$ objective. Five fields were photographed from each pup lung and were randomly numbered in a blind fashion; fields predominantly occupied with portions of large bronchi or vessels were not counted. A certified pathologist assessed the photographs, recording the highest degree of fibrosis in every field according to a modified Ashcroft scale,[39] in which fibrosis was scored using a 9-grade scale. Grade 0 indicated no fibrotic burden in the smallest fibers in the alveolar walls and normal lungs. Grade 1 denoted isolated light fibrotic changes, a septum
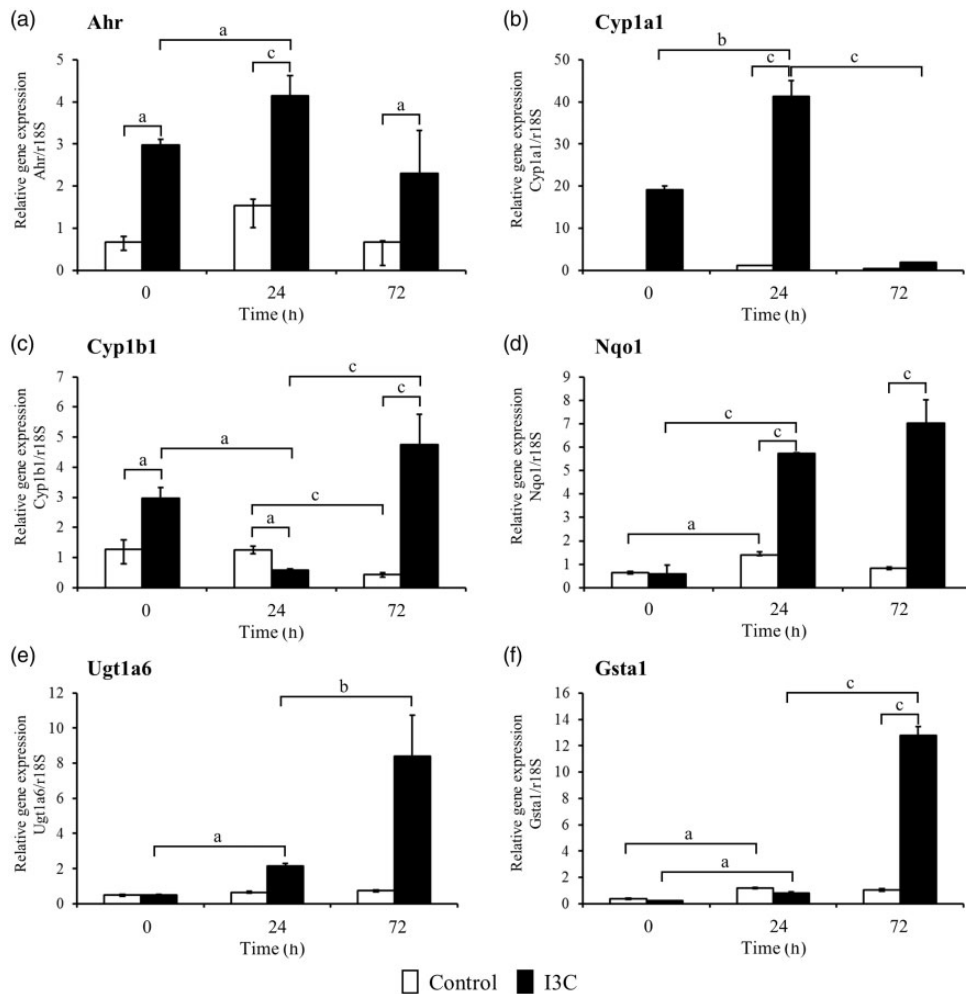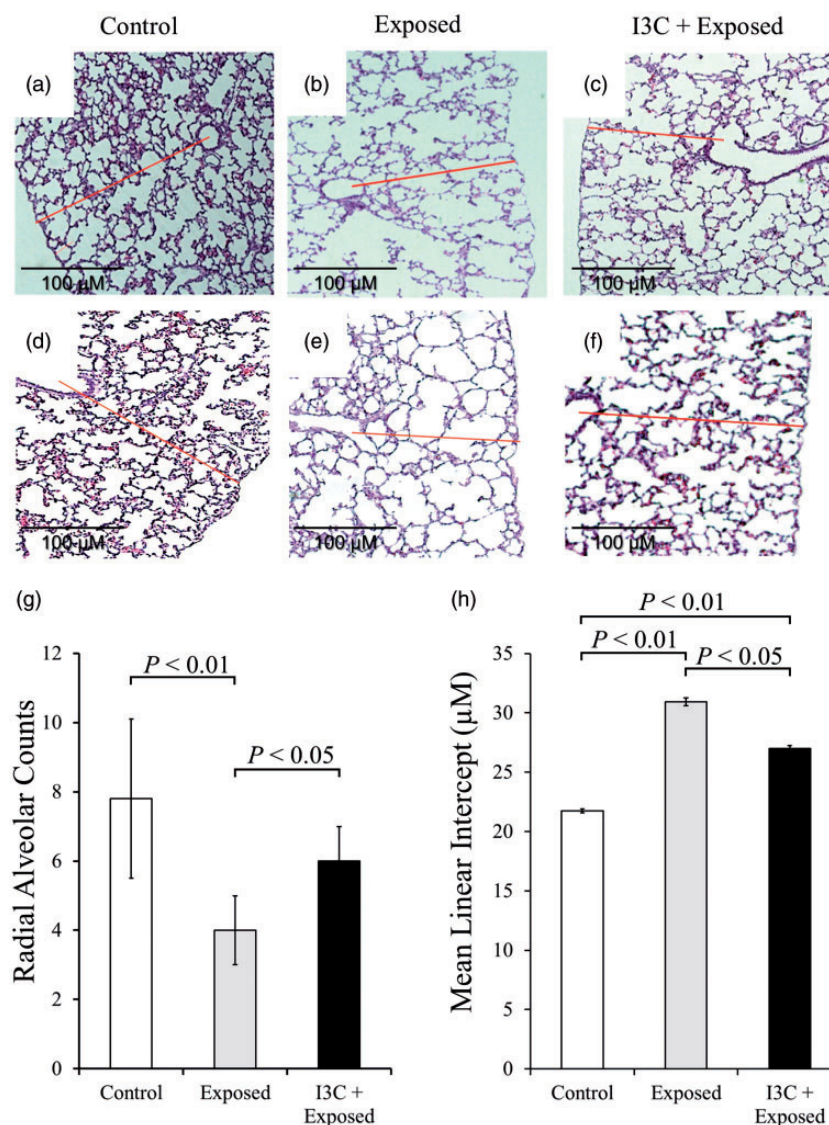

Figure 2. Effect of I3C prenatal administration in relative gene expression of *AhR* (a), *Cyp1a1* (b), *Cyp1b1* (c), *Nqo1* (d), *Ugt1a6* (e), and *Gsta1* (f) in both experimental groups: control group (open bars; pups exposed to 21% O_2; $n = 16$) and I3C group (closed bars; pups from pregnant dams administered with 100 mg/kg of I3C and exposed to 21% O_2; $n = 16$). All genes were evaluated at 0, 24, and 72 h after birth in rat pup lungs. [a]$P < 0.05$, [b]$P < 0.01$, and [c]$P < 0.001$.

less than or equal to three times thicker than normal, and alveoli partly enlarged and rarefied but without fibrotic masses present. Grade 2 indicated clearly fibrotic changes with a septum more than three times thicker than normal with knot-like formations that were not connected to each other and partly enlarged and rarefied alveoli without fibrotic masses. Grade 3 indicated contiguous fibrotic walls and a septum more than three times thicker than normal. Grade 4 signified the presence of separate fibrotic masses. Grade 5 indicated confluent fibrotic masses in >10%, but <50%, of the microscopic fields. Grade 6 denoted the presence of fibrotic masses in >50% of the fields. Grade 7 signified the presence of nearly obliterated alveoli by fibrous masses but still with up to five air

bubbles. Grade 8 indicated the complete obliteration of alveoli by fibrous masses.[39]

Statistical analysis

Data are expressed as mean ± standard deviation. Significance was determined by Student's *t*-test or a one-way ANOVA, followed by Tukey's test. Differences were statistically significant if *P* was less than 0.05. The statistical analysis was performed using IBM-SPSS Statistics software (version 22; IBM Corporation, Armonk, NY, USA). For the cytokine antibody array membrane, normalized background-corrected spot values from all the membranes were processed using R programming language 2.

Figure 3. Effect of prenatal I3C administration on radial alveolar counts (RACs) and media linear interception (MLI) in newborn rats exposed to hyperoxia–hypoxia cycles. Histopathological analysis in formalin-fixed rat lungs stained with hematoxylin and eosin on postnatal day 13 (magnification 10×): (a and d) control group (air environment 21% O_2; $n = 10$), (b and e) untreated exposed group (80%–10%–21% O_2; $n = 11$), and (c and f) exposed group treated with I3C (100 mg/kg; 80%–10%–21% O_2; $n = 7$). Representative images from two different rats are included. The red line, from the center of the respiratory bronchiole to the nearest interlobular septa, counts each bisected saccule. (g) Graphic representation of mean ± SEM for RAC of each group, in which the *P* value is depicted. (h) Graphic representation of mean ± SEM for MLI of each group, in which the *P* value is depicted. (A color version of this figure is available in the online journal.)

Spot values were transformed using a $\log_2$ scale. Cytokine differential expression between samples was calculated using paired two-tailed *t*-tests. Differences among samples were deemed significant with *P* values of <0.05.

Results

Effect of hyperoxia–hypoxia cycles and I3C treatment on weight gain

To determine the effect of hyperoxia–hypoxia cycles and I3C treatment in neonatal rats, the body weight was recorded until day 13 of life and compared within each age studied. We found that neonatal rats exposed to hyperoxia–hypoxia had a lower mean body weight (20 ± 1 g) compared with control pups (25 ± 3 g; $P < 0.05$). When pregnant dam rats were treated with I3C and pups were exposed to hyperoxia–hypoxia cycles, the mean body weight of the offspring was a quite similar to that of the exposed group (22 ± 1 g) but they did not reach to the control group ($P > 0.05$; Figure 1(b)).

Activation of AhR-dependent genes by I3C

To determine if prenatal activation of AhR-dependent genes in rat pup lungs was sustained at 0, 24, and 72 h after birth, AhR-related genes (*AhR*, *Cyp1a1*, *Cyp1b1*, *Nqo1*, *Ugt1a6*, *Gsta1*, *Aldh1a1*, and *Aldh1a3*) were quantified by RT-qPCR assays (Figure 2). Previously, to evaluate the effect of corn oil on genetic expression, the expression levels of the *Ahr* and *Cyp1a1* genes were compared in a group without treatment and another treated with corn oil. No significant differences were observed between the expression of Ahr and Cyp1a1 between the groups during 72 h of evaluation (data not shown), then the group of animals treated with corn oil was used as control in the subsequent experiments. The *AhR* gene expression was found to be twofold higher in the I3C group than that in the control group at birth ($P < 0.05$), and this effect was higher at 24 h, followed by a drop at 72 h (Figure 2(a)). In a similar pattern, the *Cyp1a1* gene expression increased 40-fold in the I3C group compared with that in the control group at 24 h ($P < 0.001$; Figure 2(b)).

The *Cyp1b1* gene expression in the I3C group exhibited an increase at birth ($P < 0.05$), followed by a reduction at 24 h and a fourfold increase after 72 h compared with that in the control group ($P < 0.01$; Figure 2(c)). The *Nqo1* gene expression levels were similar at birth in both groups; however, at 24 and 72 h after birth, these levels were significantly higher than those in the control group ($P < 0.01$; Figure 2(d)).

The *Ugt1a6* and *Gsta1* gene expression levels followed a similar pattern in the I3C group, indicating a 7-fold (Figure 2(e)) and 11-fold (Figure 2(f)) increase at 72 h compared with those in the control group ($P < 0.01$ and $P < 0.001$), respectively. The *Aldh1a1 and Aldh3a1* gene expression levels did not differ significantly between the experimental groups (data not shown).

These results indicate that I3C, when prenatally administered to dams, activates AhR-dependent genes in exposed pups.

The effect of hyperoxia–hypoxia exposure on lung histopathology

Histopathological examination of lung sections in pups exposed to hyperoxia–hypoxia cycles revealed histological signs of alveolar arrest, poor alveolar septation, and enlarged terminal air sacs (Figure 3(a) to (f)). The mean RAC was significantly lower, as expected,[5] in the exposed group (4.0 ± 1.0) compared with that in the control group (8.0 ± 2.0; $P < 0.01$; Figure 3(g)). Pups from the exposed group treated with I3C presented an increase in the mean RAC (6.0 ± 1.0) compared with untreated exposed pups ($P < 0.05$; Figure 3(g)); meanwhile, the MLI was higher in the exposed group (30.90 ± 0.329 μm) than control group
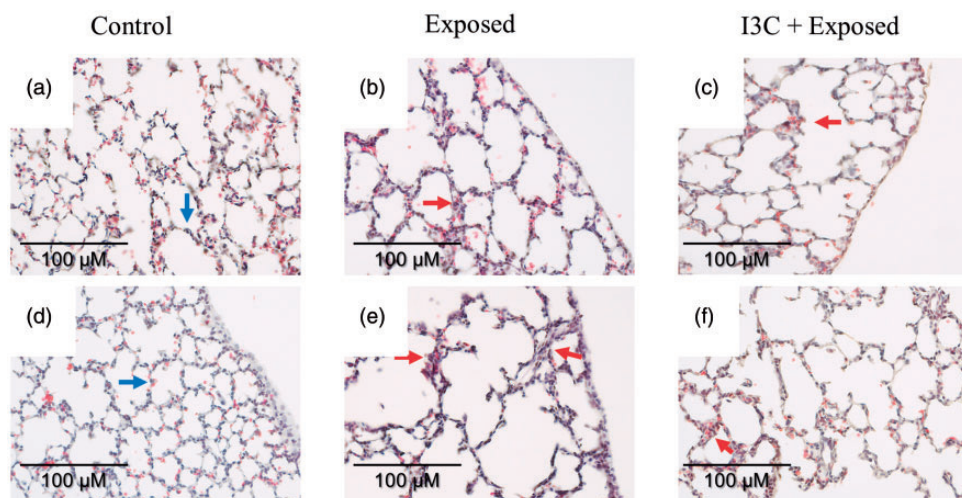
Figure 4. Fibrotic changes by prenatal I3C administration in the lungs of newborn rats exposed to hyperoxic–hypoxic cycles. Histopathological analysis of formalin-fixed rat lungs stained with Masson's trichrome on postnatal day 13 (magnification 20×): blue arrows indicate normal lung structure, and red arrows denote isolated alveolar septa with gentle fibrotic changes. Control group (a and d) (air environment of 21% O_2; $n = 5$), (b and e) untreated exposed group (80%–10%–21% O_2; $n = 5$), and (c and f) exposed group treated with I3C (100 mg/kg; 80%–10%–21% O_2; $n = 5$). Five fields were photographed for each pup and were randomly numbered in a blind fashion; fields predominantly occupied by portions of large bronchi or vessels were not counted. (A color version of this figure is available in the online journal.)

Table 2. Main findings of fibrosis by hyperoxia-hypoxia cycles and I3C treatment.

Group	Fibrosis scoring
Control	Predominately normal lung architecture.
Exposed	Fibrosis alveolar septa: clearly fibrotic changes (septum >3× thicker than normal) with knot-like formation but not connected to each other lung structure, alveoli partly enlarged and rarefied but no fibrotic masses.
I3C + Exposed	Predominately normal lung architecture.

$(21.74 \pm 0.1843 \, \mu m; P < 0.01)$. Pups from the exposed group treated with I3C presented a decrease in the mean MLI $(27 \pm 0.23 \, \mu m)$ compared with untreated exposed pups $(P < 0.05$; Figure 3(h)). Additionally, in four individual pups of the exposed group, moderate emphysema was found but was less common in pups from the I3C group; it was not present in pups from the control group (data not shown). Additionally, approximately 60% of individuals in the exposed group presented peribronchial edemas, hemorrhages, interstitial or alveolar infiltrates (mainly lymphocytes and macrophages and rarely neutrophils), or bronchial hyperplasia, but pups from the I3C group did not present any of these alterations (data not shown).

In the fibrosis analysis, no field exhibited a fibrosis degree greater than one, according to the modified Aschroft scale (Figure 4(a) to (f)). The severity of the lesions varied from one region to another with the spectrum of microscopic fields ranging from normal lung to complete fibrosis. Lung sections from control animals revealed predominately normal lung architecture (grade 0). In the exposure animals group, we observed fibrosis alveolar septa, clear fibrotic changes (septum >3× thicker than normal) with knot-like formation but not connected to each other lung structure; alveoli partly enlarged and rarefied, but no fibrotic masses (grade 1), and when the animals were treated with I3C compound they showed a pattern similar to the control group (grade 0; Table 2). Some pups showed cell conglomerates rather than an increase in the extracellular matrix. However, further studies are needed to confirm this effect and whether it is dependent on the evaluation time.

Effect of I3C on inflammatory cytokines

Additionally, to elucidate the anti-inflammatory effect of I3C, a cytokine antibody array membrane was employed to analyze plasma samples from pups six days after birth (supplementary material). We choose P6 due to the equivalence in the saccular stage in preterm human infants.[6] The results indicated that the expression of eight inflammatory mediators (tumor necrosis factor-alpha (TNFα), interleukin-13 (IL-13), vascular endothelial growth factor (VEGF), L-selectin, monocyte chemoattractant protein 1 (MCP1), agrin, IL-1R6, and tissue inhibitor of metalloproteinase 1 (TIMP1) were repressed in the exposed group compared with that in the control group; however, only L-selectin, MCP1, agrin, IL-1R6, and TIMP1 were statistically significant ($P < 0.05$), and the expression of these proteins was recovered by treatment (Figure 5(a)). Other proteins, such as leptin and IL-4, were upregulated in the exposed group, and they reached values of 30- and 180-fold, respectively, in the I3C group ($P < 0.05$; Figure 5(b)). Fractalkine expression was downregulated to <10% in the exposed group and 1% in the I3C group ($P < 0.05$) with respect to that in the control group. Although matrix metallopeptidase 8 (MMP-8), IL-2, and IL-6 were upregulated in the I3C group ($P < 0.01$), they were not modified in the exposed group.

Discussion

This study aimed to test the hypothesis that treatment of pregnant rats with I3C, an AhR inducer, would protect their offspring from hyperoxia- and hypoxia-induced lung injury. Oxygen toxicity in the lungs is mediated by ROS, and these molecules participate in both abnormal and normal signaling pathways, such as cell growth, differentiation, and inflammatory response.[40] However, when ROS production exceeds the antioxidant capacity of the cells, oxidative stress ensues, producing cellular and tissue damage through lipid peroxidation, DNA damage, and protein oxidation; thus, there are important antioxidant enzymatic lung defenses (e.g., superoxide dismutase [SOD], catalase, and glutathione peroxidase).[40] The antioxidant system is relatively deficient in immature neonates, making them more vulnerable to oxidative stress.[41] For this reason, the activation or overexpression of these antioxidant systems in the first days of life has been studied in animal hyperoxia–hypoxia models. Overexpression of extracellular SOD in the respiratory epithelial cells of newborn mice exposed to hyperoxia improves survival and preserves the proliferation of type II alveolar cells.[42,43] Nevertheless, another way to activate antioxidant enzymes is through modulation of the AhR, since its activation, also regulated by Nrf2, increases the expression of phase I and phase II enzymes (e.g., the CYP450 and NQO1).[44] The function of AhR in rodents exposed to hyperoxia has been previously reported. AhR-mediated signaling protects newborn mice from hyperoxic damage by facilitating endothelial and epithelial cell proliferation and thereby mitigating the disruption of alveorization and vascularization.[45,46]

This study confirms that I3C activates the antioxidant system in exposed pups through the transplacental barrier, activating AhR signaling pathway and supporting the hypothesis that prenatal activation of protective and antioxidant enzymes may play a role in oxidative stress diseases. It has been found that I3C in the diet of pregnant females results in the appearance of I3C metabolites in the liver of mothers and neonates, provoking the induction of the Cyp1a1 and Cyp1b1 genes.[47] In addition, our results are similar to those demonstrating the effects of other CYP450 inducers in pups from pre-treated mice with β-naphthoflavone (βNF) and exposed to postnatal hyperoxia[48] as well as to those demonstrating the protective effect of βNF in adult rats with acute lung injury.[22,49] Additionally, I3C has suppressed immune cell infiltration and pro-inflammatory cytokine production (IL-1b, IL-6, and TNFα) in a mouse model of lipopolysaccharide-
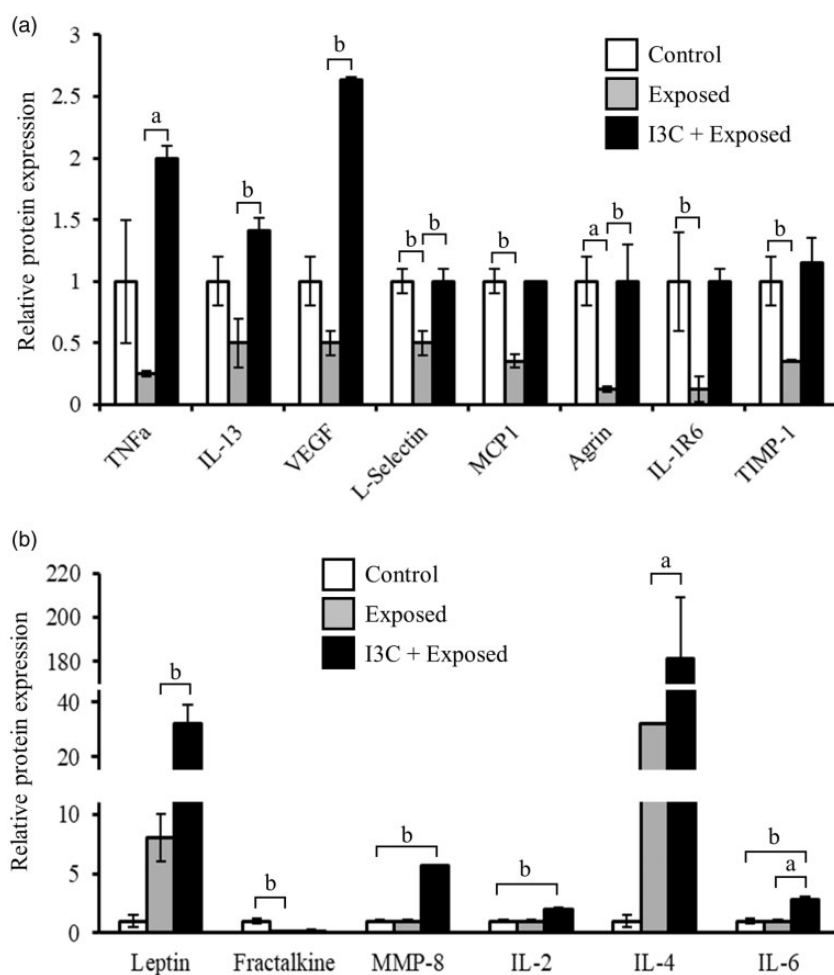
Figure 5. Comparison of cytokine expression levels through an inflammation antibody array. The levels of cytokine expression are relative to the expression of the control group. Membranes were probed with plasma protein extracts from control pups (white bars), pups exposed to hyperoxia–hypoxia cycles (gray bars), and pups from the exposed group treated with I3C (black bars). (a) Quantification of the signals (spots by duplicates) of eight candidate targets for which the control group exhibited significant downregulation compared with the exposed pups, but its expression was recovered by I3C treatment (TNFα, IL-13, VEGF, L-selectin, MCP1, agrin, IL-1R6, and TIMP1). (b) Quantification of the signals (spots by duplicates) of six candidate targets for which expression in the untreated exposed or I3C-treated group increased (leptin, MMP-8, IL-2, IL-4, and IL-6) or decreased (fractalkine) compared with that in the control group. [a]$P < 0.01$ and [b]$P < 0.05$.

induced acute lung injury.[50] Hyperoxia alone has induced *Cyp1a1* and *Cyp1a2* activation in the lungs and liver, probably via AhR-mediated mechanisms involving endogenous ligands for the AhR.[21,48,51]

We observed that pups in both the I3C group and exposed group had less body weight gain than those in the control group. In this study, I3C was suspended in corn oil (with a high n-6/n-3 ratio). Corn oil is one of the most common vehicles used in animal studies. It is known that this kind of oil increases the fat content and enhances the cytochrome P-450 activity as other enzymes.[52] Corn oil could aggravate lipid peroxidation in animals because its composition contains a high proportion of omega-6 PUFAs, but this condition has been associated with high concentration of corn oil in the diet (more than 20%).[53] Nevertheless, the corn oil doses used in this study are comparable with a standard diet for rodents.

The histological analysis confirmed that I3C-treated pups that were exposed to hyperoxia–hypoxia cycles had higher RAC and less MLI than untreated exposed pups, demonstrating that I3C attenuates lung damage from

oxygen exposure. Moreover, a degree of fibrosis greater than one was not found,[39] possibly owing to the short duration of the experiment (12 days), since fibrosis model studies have indicated that fibroproliferation occurs 2–14 days after the insult and fibrosis is established 14–28 days later.[54] In the present study, rat pups were sacrificed after 12 days of hyperoxia–hypoxia exposure, and it is conceivable that in this period, fibrosis was not yet established. Notably, in the I3C-exposed group, the percentage of animals with fibrosis was lower than that in the control group, indicating a relationship between the AhR and transforming growth factor beta (TGF-β) signaling pathways. Although human and mouse TGF-β promoters do not have canonical AhR response motifs, ligand-induced AhR activation represses TGF-β2 transcription and induces PAI-1 and PAI-2 expression, which may further suppress TGF-β signaling, hence diminishing fibrosis deposition.[55] Another study found that TGF-β levels are overexpressed in mouse embryonic fibroblasts from AhR-null mice, revealing that overactivation of the AhR in mouse embryonic fibroblasts reduces the levels of TGF-β1.[56] These, and our findings, suggest that
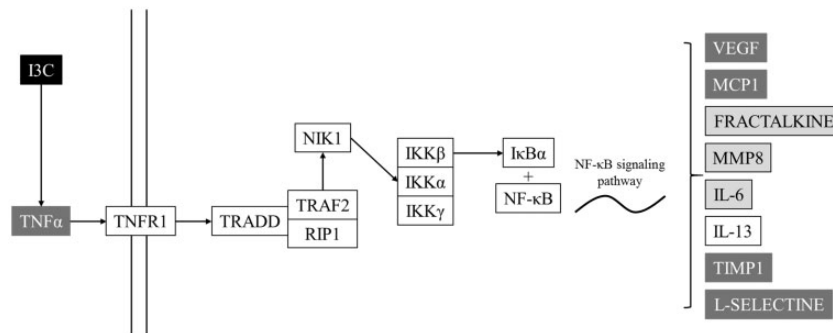
Figure 6. Hypothetical scheme of I3C effect on the inflammation process induced by hyperoxia–hypoxia cycles. Tumor necrosis factor-alpha (TNFα) can induce the inflammation process through its receptor, TNFR1, which mediates the association of some adaptor proteins, such as TRADD or TRAF2, which, in turn, initiate the recruitment of signal transducers. TNFR1 signaling activates several genes controlled by the NF-κB pathway. Protein names in dark gray boxes (VEGF, MCP1, TIMP1, L-selectin, and TNFα) were upregulated, whereas genes in light gray boxes (fractalkine, MMP-8, and IL-6) were downregulated by I3C. Adapted from https://www. kegg.jp/kegg-bin/highlight_pathway?scale=1.0&map=map04668&keyword=TNF%20cytokines

activation of the AhR by I3C in newborn rats could reduce fibrosis caused by hyperoxia–hypoxia exposure, thus improving alveolarization. An anti-inflammatory response of I3C was evaluated, in an exploratory way, by an array of cytokines, including those associated with T cell subsets and those regulated by NF-κB, which is a central cellular mediator of inflammation and is linked to the pathogenesis of BPD.[57] The main modified proteins were those involved in the regulation of the NF-κB signaling pathway (Figure 6). We hypothesized that I3C activates TNFα and thus activates the NF-κB pathway, which promotes the expression of VEGF, MCP1, TIMP1, L-selectin, MMP-8, IL-6, and IL-13, and represses fractalkine expression. The higher levels of TNFα in the I3C-treated group could be explained by the fact that NF-κB increases TNFα expression. We also hypothesized that I3C can promote T helper type (Th2) cells, which secrete IL-4. Finally, although TNFα is a well-known cytokine inductor, the high level of IL-4 observed, compared with the pro-inflammatory cytokines, had a protective effect on BPD. Accordingly, previous studies have shown a beneficial effect of I3C on the levels of pro-inflammatory mediators and the expression of some cytokines.[58,59]

The present model, unlike those used in other studies, uses periods of hypoxia (with the fraction of inspired oxygen at 10%) that increase the deleterious effects of hyperoxia,[60] which we believe creates a better approximation to the clinical scenario faced by human preterm infants during intensive care.

The I3C could be considered as a possible preventive agent that permits the NF-κB activation. This has shown promise in clinical trials aimed at preventing BPD. However, it is necessary to demonstrate in the near future the effect of I3C treatment on the activation of NF-κB for a better understanding the health benefits in premature newborns.

The authors recognize that this study has several limitations. The determination of the inflammatory cells number, evaluation of oxidative stress, evaluation of generation of mucous associated to I3C treatment,[61] and the confirmation of levels of interleukins, including to NF-κB and TGF-β, in the bronchoalveolar lavage fluid a large number of animals are necessary to strengthen our conclusions. Then, additional studies are needed to evaluate the molecular mechanisms involved in the development of lung damage and the effect of I3C in newborn rats.

Conclusions

In summary, we propose that oral administration of AhR ligands is safe for pregnant rats and increases the activity of antioxidant enzymes in their puppies, resulting in a decrease in pulmonary lesion induced by hyperoxia–hypoxia, thus improving alveolarization and RAC and decreasing fibrosis. Our findings are consistent with the concept that a functional response of AhR to harmless dietary substrates during pregnancy can protect against pulmonary injury induced by hyperoxia–hypoxia.

ORCID iDs

Víctor J Lara-Díaz https://orcid.org/0000-0002-1498-8561
Fabiola Castorena-Torres https://orcid.org/0000-0002-1157-0004

REFERENCES

1. Davidson LM, Berkelhamer SK. Bronchopulmonary dysplasia: chronic lung disease of infancy and long-term pulmonary outcomes. *J Clin Med* 2017;**6**:4

2. Chess PR, D'Angio CT, Pryhuber GS, Maniscalco WM. Pathogenesis of bronchopulmonary dysplasia. *Semin Perinatol* 2006;**30**:171–8

3. Saugstad OD. Bronchopulmonary dysplasia-oxidative stress and antioxidants. *Semin Neonatol* 2003;**8**:39–49

4. Berkelhamer SK, Farrow KN. Developmental regulation of antioxidant enzymes and their impact on neonatal lung disease. *Antioxid Redox Signal* 2014;**21**:1837–48

5. Ratner V, Slinko S, Utkina-Sosunova I, Starkov A, Polin RA, Ten VS. Hypoxic stress exacerbates hyperoxia-induced lung injury in a neonatal mouse model of bronchopulmonary dysplasia. *Neonatology* 2009;**95**:299–305

6. O'Reilly M, Thebaud B. Animal models of bronchopulmonary dysplasia. The term rat models. *Am J Physiol Lung Cell Mol Physiol* 2014;**307**: L948–58

7. Burbach KM, Poland A, Bradfield CA. Cloning of the Ah-receptor cDNA reveals a distinctive ligand-activated transcription factor. *Proc Natl Acad Sci U S A* 1992;**89**:8185–9

8. Sogawa K, Fujii-Kuriyama Y. Ah receptor, a novel ligand-activated transcription factor. *J Biochem* 1997;**122**:1075–9

9. Beischlag TV, Luis Morales J, Hollingshead BD, Perdew GH. The aryl hydrocarbon receptor complex and the control of gene expression. *Crit Rev Eukaryot Gene Expr* 2008;**18**:207–50

10. Denis M, Gustafsson JA, Wikstrom AC. Interaction of the $Mr = 90,000$ heat shock protein with the steroid-binding domain of the glucocorticoid receptor. *J Biol Chem* 1988;**263**:18520–3

11. Carver LA, Bradfield CA. Ligand-dependent interaction of the aryl hydrocarbon receptor with a novel immunophilin homolog in vivo. *J Biol Chem* 1997;**272**:11452–6

12. Hord NG, Perdew GH. Physicochemical and immunocytochemical analysis of the aryl hydrocarbon receptor nuclear translocator: characterization of two monoclonal antibodies to the aryl hydrocarbon receptor nuclear translocator. *Mol Pharmacol* 1994;**46**:618–26

13. Pollenz RS, Sattler CA, Poland A. The aryl hydrocarbon receptor and aryl hydrocarbon receptor nuclear translocator protein show distinct subcellular localizations in Hepa 1c1c7 cells by immunofluorescence microscopy. *Mol Pharmacol* 1994;**45**:428–38

14. Schulte KW, Green E, Wilz A, Platten M, Daumke O. Structural basis for aryl hydrocarbon receptor-mediated gene activation. *Structure* 2017;**25**:1025–33

15. Rushmore TH, Pickett CB. Transcriptional regulation of the rat glutathione S-transferase Ya subunit gene. Characterization of a xenobiotic-responsive element controlling inducible expression by phenolic antioxidants. *J Biol Chem* 1990;**265**:14648–53

16. Favreau LV, Pickett CB. Transcriptional regulation of the rat NAD(P)H: quinone reductase gene. Identification of regulatory elements controlling basal level expression and inducible expression by planar aromatic compounds and phenolic antioxidants. *J Biol Chem* 1991;**266**:4556–61

17. Emi Y, Ikushiro S, Iyanagi T. Xenobiotic responsive element-mediated transcriptional activation in the UDP-glucuronosyltransferase family 1 gene complex. *J Biol Chem* 1996;**271**:3952–8

18. Fujisawa-Sehara A, Sogawa K, Yamane M, Fujii-Kuriyama Y. Characterization of xenobiotic responsive elements upstream from the drug-metabolizing cytochrome P-450c gene: a similarity to glucocorticoid regulatory elements. *Nucleic Acids Res* 1987;**15**:4179–91

19. Couroucli XI, Welty SE, Geske RS, Moorthy B. Regulation of pulmonary and hepatic cytochrome P4501A expression in the rat by hyperoxia: implications for hyperoxic lung injury. *Mol Pharmacol* 2002;**61**:507–15

20. Chen C, Kong AN. Dietary chemopreventive compounds and ARE/EpRE signaling. *Free Radic Biol Med* 2004;**36**:1505–16

21. Jiang W, Welty SE, Couroucli XI, Barrios R, Kondraganti SR, Muthiah K, Yu L, Avery SE, Moorthy B. Disruption of the Ah receptor gene alters the susceptibility of mice to oxygen-mediated regulation of pulmonary and hepatic cytochromes P4501A expression and exacerbates hyperoxic lung injury. *J Pharmacol Exp Ther* 2004;**310**:512–9

22. Shivanna B, Zhang W, Jiang W, Welty SE, Couroucli XI, Wang L, Moorthy B. Functional deficiency of aryl hydrocarbon receptor augments oxygen toxicity-induced alveolar simplification in newborn mice. *Toxicol Appl Pharmacol* 2013;**267**:209–17

23. Schwartz E, Zelig R, Parker A, Johnson S. Vitamin a supplementation for the prevention of bronchopulmonary dysplasia in preterm infants: an update. *Nutr Clin Pract* 2017;**32**:346–53

24. Guthrie G, Premkumar M, Burrin DG. Emerging clinical benefits of new-generation fat emulsions in preterm neonates. *Nutr Clin Pract* 2017;**32**:326–36

25. Leibelt DA, Hedstrom OR, Fischer KA, Pereira CB, Williams DE. Evaluation of chronic dietary exposure to indole-3-carbinol and absorption-enhanced 3,3'-diindolylmethane in Sprague-Dawley rats. *Toxicol Sci* 2003;**74**:10–21

26. Ampofo E, Lachnitt N, Rudzitis-Auth J, Schmitt BM, Menger MD, Laschke MW. Indole-3-carbinol is a potent inhibitor of ischemia-reperfusion-induced inflammation. *J Surg Res* 2017;**215**:34–46

27. Borger JG, Lau M, Hibbs ML. The influence of innate lymphoid cells and unconventional T cells in chronic inflammatory lung disease. *Front Immunol* 2019;**10**:1597

28. Garth J, Barnes JW, Krick S. Targeting cytokines as evolving treatment strategies in chronic inflammatory airway diseases. *Int J Mol Sci* 2018;**19**:3402

29. *Australian code for the care and use of animals for scientific purposes.* 8th ed. National Health and Medical Research Council, 2013, https://www.nhmrc.gov.au/about-us/publications/australian-code-care-and-use-animals-scientific-purposes#toc__1833 (2013, accessed 9 October 2020).

30. Anesthesia (Guideline). Vertebrate Animal Research of Iowa University, USA, https://animal.research.uiowa.edu/iacuc-guidelines-anesthesia (2020, accessed 9 October 2020).

31. Ratner V, Kishkurno SV, Slinko SK, Sosunov SA, Sosunov AA, Polin RA, Ten VS. The contribution of intermittent hypoxemia to late neurological handicap in mice with hyperoxia-induced lung injury. *Neonatology* 2007;**92**:50–8

32. Livak KJ, Schmittgen TD. Analysis of relative gene expression data using real-time quantitative PCR and the 2(-Delta Delta C(T)) method. *Methods* 2001;**25**:402–8

33. Funkhouser WK. Chapter 9: Pulmonary pathology. In: Reisner HM (ed.) *Pathology: a modern case study.* 2nd ed. New York, NY: McGraw-Hill, 2020.

34. Coalson JJ. Pathology of bronchopulmonary dysplasia. *Semin Perinatol* 2006;**30**:179–84

35. Kemp WL, Burns DK, Brown TG. *Pathology: the big picture.* New York, NY: McGraw-Hill, 2008.

36. Emery JL, Mithal A. The number of alveoli in the terminal respiratory unit of man during late intrauterine life and childhood. *Arch Dis Child* 1960;**35**:544–7

37. Matute-Bello G, Downey G, Moore BB, Groshong SD, Matthay MA, Slutsky AS, Kuebler WM; Group ALIiAS. An official American Thoracic Society workshop report: features and measurements of experimental acute lung injury in animals. *Am J Respir Cell Mol Biol* 2011;**44**:725–38

38. Crowley G, Kwon S, Caraher EJ, Haider SH, Lam R, Batra P, Melles D, Liu M, Nolan A. Quantitative lung morphology: semi-automated measurement of mean linear intercept. *BMC Pulm Med* 2019;**19**:206

39. Hubner RH, Gitter W, El Mokhtari NE, Mathiak M, Both M, Bolte H, Freitag-Wolf S, Bewig B. Standardized quantification of pulmonary fibrosis in histological samples. *Biotechniques* 2008;**44**:50711

40. Buczynski BW, Maduekwe ET, O'Reilly MA. The role of hyperoxia in the pathogenesis of experimental BPD. *Semin Perinatol* 2013;**37**:69–78

41. Hilgendorff A, Ma O. Bronchopulmonary dysplasia early changes leading to long-term consequences. *Front Med* 2015;**2**:1–10

42. Auten RL, O'Reilly MA, Oury TD, Nozik-Grayck E, Whorton MH. Transgenic extracellular superoxide dismutase protects postnatal alveolar epithelial proliferation and development during hyperoxia. *Am J Physiol Lung Cell Mol Physiol* 2006;**290**:L32–40

43. Wispe JR, Warner BB, Clark JC, Dey CR, Neuman J, Glasser SW, Crapo JD, Chang LY, Whitsett JA. Human Mn-superoxide dismutase in pulmonary epithelial cells of transgenic mice confers protection from oxygen injury. *J Biol Chem* 1992;**267**:23937–41

44. Shivanna B, Zhang S, Patel A, Jiang W, Wang L, Welty SE, Moorthy B. Omeprazole attenuates pulmonary aryl hydrocarbon receptor activation and potentiates hyperoxia-induced developmental lung injury in newborn mice. *Toxicol Sci* 2015;**148**:276–87

45. Bhattacharya S, Zhou Z, Yee M, Chu CY, Lopez AM, Lunger VA, Solleti SK, Resseguie E, Buczynski B, Mariani TJ, O'Reilly MA. The genome-wide transcriptional response to neonatal hyperoxia identifies AhR as a key regulator. *Am J Physiol Lung Cell Mol Physiol* 2014;**307**:L516–23

46. Shivanna B, Maity S, Zhang S, Patel A, Jiang W, Wang L, Welty SE, Belmont J, Coarfa C, Moorthy B. Gene expression profiling identifies cell proliferation and inflammation as the predominant pathways regulated by aryl hydrocarbon receptor in primary human fetal lung cells exposed to hyperoxia. *Toxicol Sci* 2016;**152**:155–68

47. Larsen-Su SA, Williams DE. Transplacental exposure to indole-3-carbinol induces sex-specific expression of CYP1A1 and CYP1B1 in the liver of Fischer 344 neonatal rats. *Toxicol Sci* 2001;**64**:162–8

48. Couroucli XI, Liang YW, Jiang W, Barrios R, Moorthy B. Attenuation of oxygen-induced abnormal lung maturation in rats by retinoic acid: possible role of cytochrome P4501A enzymes. *J Pharmacol Exp Ther* 2006;**317**:946–54

49. Sinha A, Muthiah K, Jiang W, Couroucli X, Barrios R, Moorthy B. Attenuation of hyperoxic lung injury by the CYP1A inducer beta-naphthoflavone. *Toxicol Sci* 2005;**87**:204–12

50. Jiang J, Kang TB, Shim DW, Oh NH, Kim TJ, Lee KH. Indole-3-carbinol inhibits LPS-induced inflammatory response by blocking TRIF-dependent signaling pathway in macrophages. *Food Chem Toxicol* 2013;**57**:256–61

51. Zhang S, Patel A, Chu C, Jiang W, Wang L, Welty SE, Moorthy B, Shivanna B. Aryl hydrocarbon receptor is necessary to protect fetal human pulmonary microvascular endothelial cells against hyperoxic injury: mechanistic roles of antioxidant enzymes and RelB. *Toxicol Appl Pharmacol* 2015;**286**:92–101

52. Takashima K, Mizukawa Y, Morishita K, Okuyama M, Kasahara T, Toritsuka N, Miyagishima T, Nagao T, Urushidani T. Effect of the difference in vehicles on gene expression in the rat liver – analysis of the control data in the toxicogenomics project database. *Life Sci* 2006;**78**:2787–96

53. Rahman KM, Sugie S, Okamoto K, Watanabe T, Tanaka T, Mori H. Modulating effects of diets high in omega-3 and omega-6 fatty acids in initiation and postinitiation stages of diethylnitrosamine-induced hepatocarcinogenesis in rats. *Jpn J Cancer Res* 1999;**90**:31–9

54. Jenkins RG, Moore BB, Chambers RC, Eickelberg O, Königshoff M, Kolb M, Laurent GJ, Nanthakumar CB, Olman MA, Pardo A, Selman M, Sheppard D, Sime PJ, Tager AM, Tatler AL, Thannickal VJ, White ES, AAoRCaM B. An official American Thoracic Society workshop report: use of animal models for the preclinical assessment of potential therapies for pulmonary fibrosis. *Am J Respir Cell Mol Biol* 2017;**56**:667–79

55. Puga A, Tomlinson CR, Xia Y. Ah receptor signals cross-talk with multiple developmental pathways. *Biochem Pharmacol* 2005;**69**:199–207

56. Kung T, Murphy KA, White LA. The aryl hydrocarbon receptor (AhR) pathway as a regulatory pathway for cell adhesion and matrix metabolism. *Biochem Pharmacol* 2009;**77**:536–46

57. Wright CJ, Kirpalani H. Targeting inflammation to prevent bronchopulmonary dysplasia: can new insights be translated into therapies?. *Pediatrics* 2011;**128**:111–26

58. Benson JM, Shepherd DM. Dietary ligands of the aryl hydrocarbon receptor induce anti-inflammatory and immunoregulatory effects on murine dendritic cells. *Toxicol Sci* 2011;**124**:327–38

59. Mohammadi S, Memarian A, Sedighi S, Behnampour N, Yazdani Y. Immunoregulatory effects of indole-3-carbinol on monocyte-derived macrophages in systemic lupus erythematosus: a crucial role for aryl hydrocarbon receptor. *Autoimmunity* 2018;**51**:199–209

60. Berger J, Bhandari V. Animal models of bronchopulmonary dysplasia. The term mouse models. *Am J Physiol Lung Cell Mol Physiol* 2014;**307**:L936–47

61. Busbee PB, Menzel L, Alrafas HR, Dopkins N, Becker W, Miranda K, Tang C, Chatterjee S, Singh U, Nagarkatti M, Nagarkatti PS. Indole-3-carbinol prevents colitis and associated microbial dysbiosis in an IL-22-dependent manner. *JCI Insight* 2020;**5**:e127551